King Saud University

Journal of Saudi Chemical Society

www.ksu.edu.sa
www.sciencedirect.com

ORIGINAL ARTICLE

Removal of lead ions using hydroxyapatite nano-material prepared from phosphogypsum waste

CrossMark

S.M. Mousa [a,*], N.S. Ammar [b], H.A. Ibrahim [b]

[a] Chemistry Dept., Science & Art College, King Abdulaziz University, Rabigh Campus, P.O. Box 344, 21911 Rabigh, Saudi Arabia
[b] Water Pollution Research Dept., National Research Centre, Dokki, P.O. Box 12622, 11787 Cairo, Egypt

Abstract   Nano-material of calcium hydroxyapatite (n-CaHAP), with particle size ranging from 50 to 57 nm which was prepared from phosphogypsum waste (PG), was used for the removal of lead ions (Pb (II)) from aqueous solutions. It was investigated in a batch reactor under different experimental conditions. Effects of process parameters such as pH, initial Pb ion concentration and adsorbent dose were studied. Also, various types of kinetic modeling have been studied where the lead uptake was quantitatively evaluated using the Langmuir, Freundlich and Dubinin–Kaganer–Radushkevich (DKR) model. The Pb ions adsorption onto n-CaHAP could best fit the Langmuir isotherm model. The maximum adsorption capacity (q_{max}) for Pb ions was 769.23 mg/g onto n-CaHAP particles.

1. Introduction

Lead (Pb) ions have been classified as a hazardous heavy metal of high priority in the perspective of human and environmental risk [1–3]. It is considered a worldwide pollutant element because it is commonly detected in several industrial wastewaters [4]. Environmental protection legislation and public environmental concerns, promote the search for novel techniques for the removal of heavy metals from industrial wastewater [5,6].

Many adsorbents have been used for the removal of lead ions from aqueous media [7,8]. These adsorbents were used in raw materials [9,10] or with modified surface [11–13]. Thus, there is a growing demand to find relatively efficient, low cost and easily available adsorbents for the adsorption of lead [14]. The adsorption process has come to the forefront as one of the major techniques for heavy metal removal from wastewaters [15,16].

Phosphogypsum (PG) is an industrial waste derived from phosphoric acid and phosphate fertilizer manufactures by using the wet method. This process is economic but results in the production of a large amount of PG [17] where, every ton of phosphoric acid produced about 5 tons of PG [18]. World PG production is variously estimated to be in the region of 100–280 Mt per year [19], so it may cause serious storage

* Corresponding author at: Chemistry Dept., Faculty of Science and Arts, King Abdulaziz Univ., Rabigh Campus, Girls Sector, Rabigh, P.O. Box 344, Rabigh 21911, Saudi Arabia. Tel.: 00966568615154; fax: 00966664232927.
E-mail address: saharmousa69@yahoo.com (S.M. Mousa).
Peer review under responsibility of King Saud University.

ELSEVIER   **Production and hosting by Elsevier**

and environmental problems [17]. In Egypt, it is used partially as a soil conditioner [20] however; hard works are made for beneficiation of PG. The complete chemical analysis of PG confirmed that the waste was free of radioactive elements and heavy metals such as Cd which is the most pollutant element which could hinder the utilization of the waste [21]. PG was converted into calcium hydroxyapatite $Ca_{10}(PO_4)_6(OH)_2$ and ammonium sulfate, where hydroxyapatite (HAP), is one of the most important constituents of the biocompatible inorganic materials used in human hard tissues (bone and teeth) [22,23]. The chemical species constituting of HAP crystals are calcium, phosphorus, oxygen and hydrogen, which are expected to have no toxicity [24]. Synthetic hydroxyapatite is a particularly attractive material, which has received considerable attention over the past two decades, for bone and tooth implants because of its chemical similarity to natural bone [25]. It is also of importance in many industrial applications, such as catalysis, ion exchange, and metal removal [26–29]. Several methods have been used for the synthesis of HAP [30–34]. So, the main goal of this work is using nanomaterials which were prepared from phosphogypsum waste [35] to remove Pb (II) from aqueous solutions.

2. Materials and methods

2.1. Preparation and determination of lead concentration

$Pb(NO_3)_2$ of analytical grade from Merck, was used in the preparation of stock standard solution (1000 mg/L). The synthetic solutions were then prepared by diluting the lead stock standard solution. The concentration of lead ions in all samples was determined using Atomic Absorption Spectrometer Varian Spectra (220) with graphite furnace accessory and equipped with deuterium arc background corrector according to the Standard Method [36].

2.2. Preparation and characterization of n-CaHAP before and after lead ion removal

Method of preparation and complete characterization of calcium hydroxyapatite calcined at 600 °C with the particle size 50–57 nm was explained and discussed previously [35].

Sample characterization before and after lead ion removal was conducted using X-ray diffraction (XDR), instrument Bruker-D8 advance instrument with CuKα1 target with a second monochromator 40 kV, 40 mA.

Determination of acidobasic properties of the n-CaHAP surface was done by using the point of zero charge pH_{pzc} method, where, 500 ml of 0.01 M NaCl solution was degassed using N_2 gas in order to remove and avoid further dissolution of carbon dioxide. Take 10 ml from 0.01 M NaCl in 10 beakers and adjust the pH ranging from 1 to 10 pH (by adding either HCl or NaOH). 10 mg of n-CaHAP was added in 10 ml of each solution with different pH. The final pH after 24 h was measured.

2.3. Batch sorption experiments

Sorption kinetic and isotherm models of n-CaHAP for Pb (II) removal were studied using the batch adsorption process. Each

of the batch adsorption studies was carried out by contacting the adsorbent with the lead ions at room temperature (25 ± 0.1 °C) in a glass bottle. A series of experiments were also conducted in order to determine the effects of pH, contact time, sorbent dosage and initial ions concentration on the adsorption of Pb (II).

Each experiment was conducted in a mechanical shaker at 120 rpm. All samples were filtered and the metal ion concentration was determined in the filtrate. To distinguish between possible metal precipitation and actual metal sorption, controls were used without adsorbent materials. Furthermore, the effect of pH on the dissolution of HA at low pH was studied.

2.4. Calculation of lead ions uptake by n-CaHAP

All experiments were carried out in triplicate and the mean of the quantitative results was used for further calculations, the percent relative standard deviation of results was calculated and if the value of standard deviation for any sample was > 3% the data were not used.

The percentage of lead ions removed by calcium n-CaHAP during the series of batch investigations was determined using the following Eq. (1) expressed as:

$$Removal\ (\%) = \frac{C_0 - C_f}{C_0} \times 100 \tag{1}$$

where C_0 and C_f are the initial and final concentrations (mg/L) of metal ions in solution, respectively.

3. Results and discussion

3.1. Characterization of n-CaHAP before and after lead ion removal

Fig. 1 shows the X-ray diffraction patterns of unloaded n-CaHAP (a) and (b) the air-dried loaded sample by Pb ions. The X-ray diffraction analysis shows structural changes in n-CaHAP after the adsorption process at 2θ (30°) due to the formation of $Ca_{(10-x)}Pb_x(PO_4)_6(OH)_2$ [37]. Furthermore, all
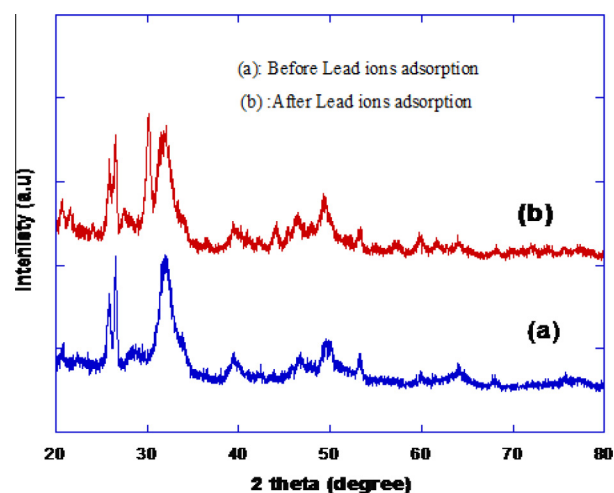

Figure 1 X-ray diffraction patterns of n-CaHAP before and after the adsorption process.

of the XRD peaks were shifted toward the lower diffraction angles (for maximum peak from $2\theta = 31.785°$ to $2\theta = 31.713°$) which means that there had been an expansion in structure. This reality could not be explained by a cation exchange mechanism, because the replacement of Pb (II) (ionic radius 0.2 Å), which is smaller than Ca (II) (ionic radius 0.99 Å) decreases unit cell dimensions and then increases 2θ values. Results of the phase identification analysis of XRD patterns of Pb-n-CaHAP particles show that the formation of a complex on the surface of n-CaHAP may be a primary mechanism of Pb ion uptake. Our results are in good agreement with other studies for the removal of metals from aqueous solution by n-CaHAP [38].

Also, the pH drift method (point of zero charge pHpzc) is used to determine the acidobasic properties of the n-CaHAP surface [39]. Fig. 2 illustrates the difference between the initial pH_0 and final pH (pH_f) values ($\Delta pH = pH_0 - pH_f$) against the pH_0. The point of intersection of the resulting curve (pH_0) gave the PZC of n-CaHAP. The PZC of n-CaHAP was found to be 3.0. This means that at pH < 3.0, the positively charged surface of the n-CaHAP is predominant, while at pH > 3.0, the negatively charged surface is predominant. pH is an important factor for determining the form of the metallic species in aqueous media. It influences the adsorption process of metal ions, as it is determined as the magnitude and sign of the charge on ions [40].

3.2. Effect of pH

The effect of solution pH on the sorption of Pb (II) from the aqueous solution using n-CaHAP was investigated in the pH range of 1.0–5.5 with the initial Pb (II) concentration of 50 mg/L. Fig. 3 reveals that the efficiency of lead ion removal increased significantly as pH increased from 1.0 to 4.5 and remains constant from 4.5 to 5.5. On studying the effect of pH on HAP, it was found that HAP dissolved by 49% at pH 1 and 16% at pH 2. However, at pH 3 there is no effect on the dissolution of HAP. Consequently, the adsorption of Pb (II) onto HAP was suppressed at the lowering pH due to the destruction of crystalline structure for the initial HAP material in the acidic conditions during the adsorption experiment [41–43].

However, by increasing the pH, the competition between positive charges decreases as these surface active sites become more negatively charged, which enhances the adsorption of the
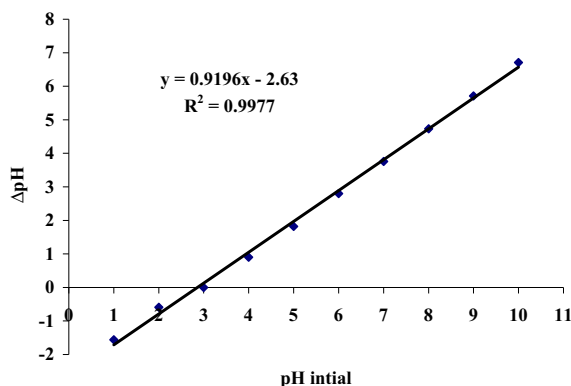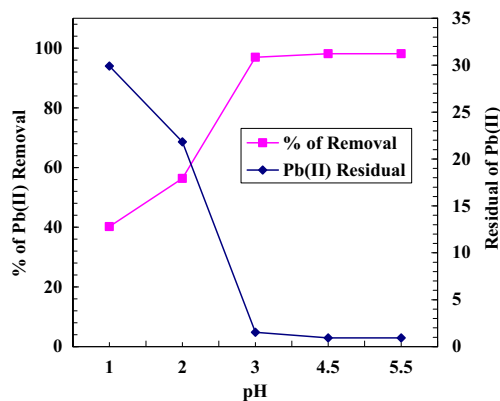

Figure 3 Lead ions removal efficiency of n-CaHAP as a function of pH solution at an initial concentration 50 mg/L, and 0.5 g/L adsorbent weight.

positively charged Pb (II) through the electrostatic force of attraction [44,45]. Thus, conducting experiments at optimum pH ranging from 4.5 to 5.5 ensures the presence of the divalent form of ions, preserves the chemical stability of the n-CaHAP and the removal efficiency for Pb (II) reached upto 98.1%.

The reason that n-CaHAP behaved differently in adsorbing Pb (II) at different solution pHs can be explained by considering the pHpzc of the adsorbent as well as the molecular nature of Pb (II). The pHpzc of n-CaHAP powders was found to be 3.0. This means that n-CaHAP powder surface was positive charged at solution pH below pH 3.0 and Pb (II) ions were repelled by n-CaHAP powder surface resulting in the reduction of Pb (II) adsorption. At pH higher than pHpzc, the surface of n-CaHAP powders can be deprotonated [46–48].

3.3. Effect of contact time

The equilibrium time is a significant effect of selecting a wastewater treatment scheme, where the time consumed for wastewater disposal should be measured. As shown in Fig. 4 the sorption of Pb (II) onto the n-CaHAP was very fast and equilibrium was reached within 5 min, where the removal percentages of lead ions reached upto 97.8%. A further increase in contact time has no effect on the removal percent. Therefore,
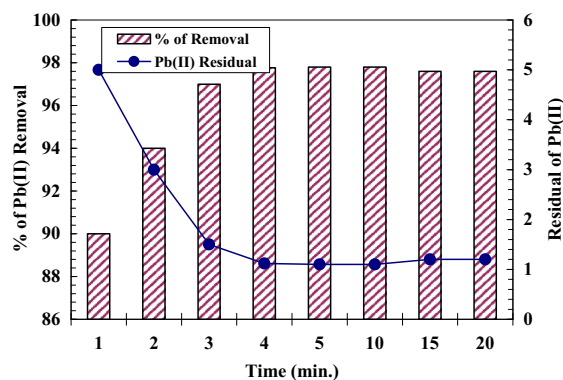

Figure 2 Point of zero charge (PZC) of n-CaHAP.

Figure 4 Effect of contact time on the removal of Pb^{2+} by adsorption onto n-CaHAP at an initial concentration 50 mg/L, at pH ranging from 4.5 to 5.5 and 0.5 g/L adsorbent weight.

5 min shaking time was considered as equilibrium time for maximum adsorption. The decrease in the rate of removal of Pb (II) with time may be due to aggregation of Pb (II) around n-CaHAP particles. This aggregation may hamper the migration of the adsorbate, as the adsorption sites become filled up, and also resistance to the diffusion of Pb (II) molecules in the adsorbents increases [49].

3.4. Kinetic modeling

3.4.1. Sorption kinetics

Kinetic characteristic in a sorbent depends on the presence of the active site and the ease of access of the Pb ions onto the active site without sterical hindrance which is greatly determined by the matrices of the sorbent. The mechanism of sorption depends on the physical and chemical characteristics of the sorbent as well as on the mass transfer process [50]. The kinetics rate of Pb ion sorption onto n-CaHAP was analyzed using pseudo first-order, pseudo-second order, Intra-particle diffusion and the Elovich kinetic model. The agreement between experimental data and the studied models are predicted by the relatively higher correlation coefficient value (R^2, values close to 1).

3.4.2. Pseudo first-order kinetic model

The kinetic data were treated with the Lagergren first-order model [51] which is the earliest known one describing the adsorption rate based on the adsorption capacity. The integral form of the pseudo first-order model is generally expressed by Eq. (2):

$$\log[q_e - q_t] = \log[q_e] - \left[\frac{K_{1,ads}}{2.303}\right]t \qquad (2)$$

where q_e (meq/g) and q_t are the amounts of adsorbed Pb ions on the sorbent at the equilibrium and at any time t, respectively; and $k_{1,ads}$ is the Lagergren rate constant of the first-order sorption (min^{-1}).

The model is based on the assumption that the rate is proportional to the number of free sites or intra-particle diffusion model. If the pseudo first-order kinetics is applicable, a plot of log ($q_e - q_t$) versus t should provide a linear relationship from which $k_{1,ads}$ and predicted q_e can be determined from the slope and intercept of the plot, respectively (Fig. 5). The variation in rate should be proportional to the first power of concentration for strict surface adsorption. However, the relationship
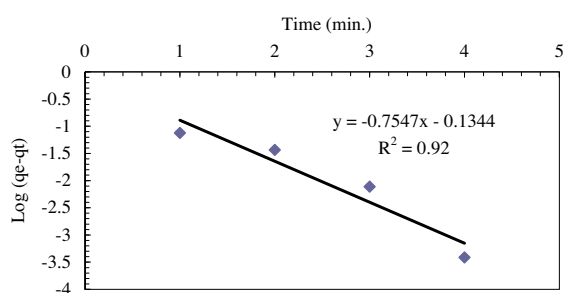
between initial solute concentration and rate of adsorption will not be linear when pore diffusion limits the adsorption process.

It was observed from Fig. 5 that first-order model failed to provide a realistic estimate of q_e of adsorbed Pb ions since the experimental values of q_e (0.944 meq/g) were higher than the fitted value (0.734 meq/g) for n-CaHAP. This underestimation of the amount of binding sites is probably due to the fact that q_e was determined from the y-intercept ($t = 0$). The intercept is most strongly affected by the short term of lead ion uptake, which is usually much lower than the equilibrium uptake. It can be concluded that the adsorption of Pb ions onto n-CaHAP is not suitable to describe the entire process and not a first-order reaction, even when the correlation coefficient R^2 is relatively high ($R^2 = 0.923$).

3.4.3. Pseudo-second order model

The pseudo-second-order model is based on the assumption that sorption follows a second-order mechanism, whereby the rate of sorption is proportional to the square of the number of unoccupied sites [52]. The linearized form of the Eq. (3) is expressed as

$$\frac{t}{q_t} = \frac{1}{K_{2,ads} * q_e^2} + \frac{t}{q_e} \qquad (3)$$

where $k_{2,ads}$ is the rate constant of second-order biosorption (g/meq min).

The linearized second-order plot of t/q_t against t (Fig. 6) according to Eq. (3) resulted in straight lines for Pb ions which led to the determination of the second-order rate constants ($k_{2,ads}$) (9.25) and q_e from the slope and y-intercept. The q_e values (0.968 meq/g) were very close to the experimentally determined ones (0.944 meq/g), which indicate the appropriateness of this model. The R^2 value of the correlation coefficient indicated that the adsorption data for Pb (II) onto n-CaHAP best fit the pseudo-second-order model. The basic hypothesis subsequent to the pseudo-second-order model designated that chemisorptions played the most important role and may control the adsorption process [53].

3.4.4. Intra-particle diffusion model

Pseudo first order and pseudo second-order models cannot recognize the diffusion mechanisms during the sorption process. In a well stirred batch adsorption system, the intraparticle diffusion model has been used to explain the adsorption
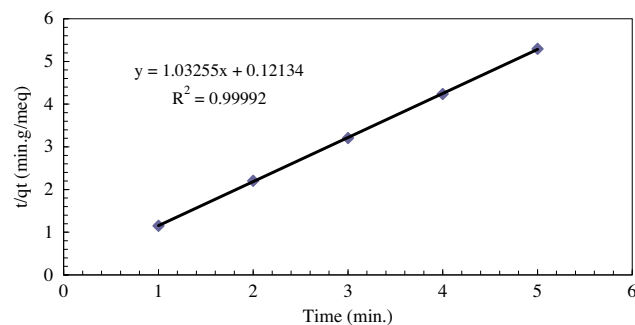

Figure 5 Pseudo-first order for the sorption of Pb (II) by n-CaHAP at 25 ± 0.2 °C, 0.5 g/L adsorbent weight and at pH ranging from 4.5 to 5.5.

Figure 6 Pseudo-second order for the sorption of Pb (II) by n-CaHAP at 25 ± 0.2 °C, 0.5 g/L adsorbent weight and at pH ranging from 4.5 to 5.5.

process occurring on a porous adsorbent. A plot of the amount of sorbate adsorbed, q_t (mg/g) and the square root of the time, gives the rate constant. It is calculated by using the intra-particle diffusion model given as Eq. (4) [54,55].

$$q_t = k_i t^{0.5} + C_i \qquad (4)$$

where q_t is the amount of Pb ions adsorbed (mg/g) at time t, k_i is the intra-particle diffusion constant (mg/g min$^{0.5}$) which indicate an enhancement in the rate of adsorption and C_i is the intercept of the line (mg/g) which is equal to the intraparticle diffusion constant. It is directly proportional to the boundary layer thickness. Fig. 7 shows multi-linearity between $t^{0.5}$ and q_t for the removal of Pb (II) by n-CaHAP. It was also found that the intra-particle diffusion of Pb (II) within n-CaHAP occurred in two stages. Explanation of these two stages was based on reports presented earlier [56], where, the linear step corresponds to fast uptake of n-CaHAP sorbate. The line in the initial stage does not pass through the origin; this means that uptake is dominated by film diffusion than for the intra-particle diffusion process. In the second stage, sorbate adsorption speeds up reflecting non consecutive diffusion of sorbate molecules into the micropores with a wider pore width within the sorbent [56]. Generally, adsorption controlled by the intraparticle model is due to the preferential adsorption of sorbate in the micropores.

3.5. Effect of adsorbent dose

As adsorption processes are mainly a surface phenomenon, therefore, adsorption efficiency can be significantly affected by surface area and available active sites due to the mass amount of adsorbent [57]. The percentage of lead ions removal at various amounts of adsorbent n-CaHAP ranging from 0.1 to 1 g/L was used (Fig. 8). At adsorbent dosage 0.3 g/L, there is no significant removal of Pb (II), as the surface of Pb ions concentration and their solution are in equilibrium with each other [58]. However, the incremental decrease in removal percent with an increase in the adsorbent dose is mainly due to unsaturation of adsorption sites through the adsorption reaction, where, the aggregation and overlapping of active sites at higher adsorbent masses lead to the decrease in the effective surface area required for sorption [59].
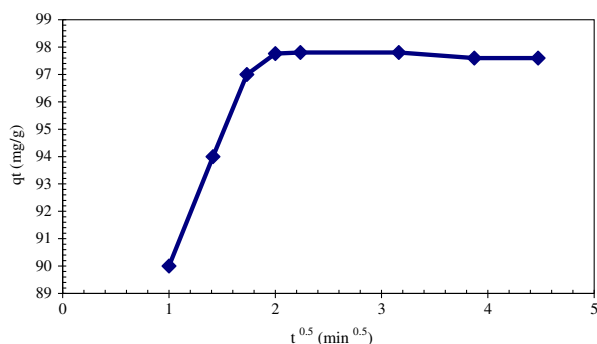

Figure 8 Effect of adsorbent dose on the removal of lead ions by n-CaHAP at 25 ± 0.2 °C, initial concentration 50 mg/L and at pH ranging from 4.5 to 5.5.
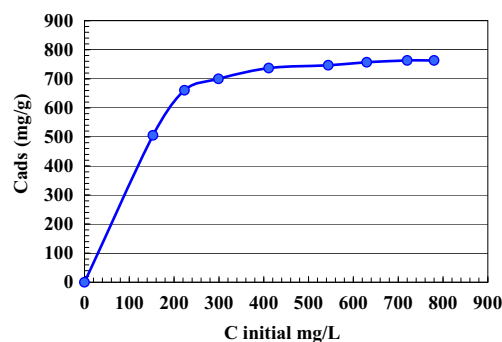
Figure 9 Effect of initial Pb (II) ions concentration on adsorption capacity of n-CaHAP at optimum operating condition.

3.6. Effect of lead ions concentration and isotherm modeling

The effect of lead ion concentrations was studied using different lead ions concentration ranges from 100 to 800 mg L^{-1} under optimum operation conditions of pH values, contact time and adsorbent dose (Fig. 9). The Pb (II) adsorption capacity of the n-CaHAP initially increased with increasing the initial Pb (II) ions concentration and reached a saturation point with a maximum equilibrium uptake (769.23 mg g^{-1}) for Pb ions. Finally, the uptake adsorption capacity did not significantly change with the initial Pb (II) ion concentration.

3.6.1. Isotherm models

Batch adsorption studies for understanding the mechanism of Pb ions adsorption on n-CaHAP by fitting the experimental records to the mainly used models included Langmuir, Freundlich and Dubinin–Kaganer–Radushkevich (DKR) adsorption isotherms [60].

The Langmuir isotherm [61] assumes monolayer adsorption onto a surface with a finite number of identified sites, and its linear form can be expressed as Eq. (5):

$$\frac{C_e}{q} = \frac{1}{K q_{max}} + \frac{C_e}{q_{max}} \qquad (5)$$

where K (L/g) is the equilibrium adsorption constant which is related to the affinity of the binding sites and q_{max} (mg/g) is the maximum amount of lead ion per unit mass of sorbent when all binding sites are occupied.

Figure 7 Intraparticle diffusion model kinetic model for removal of Pb (II) by n-CaHAP at 25 ± 0.2 °C, 0.5 g/L adsorbent weight and at pH ranging from 4.5 to 5.5.
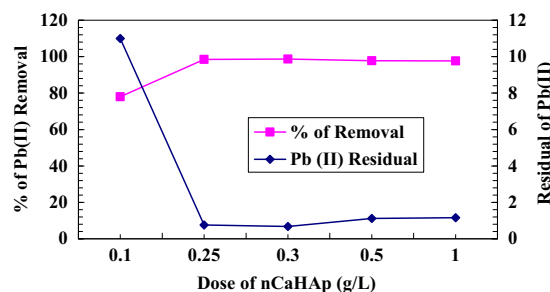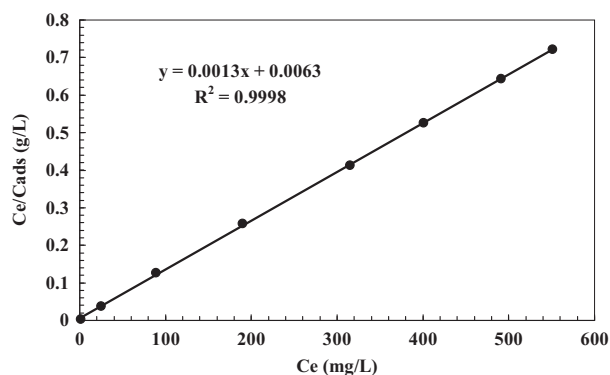
Table 1 Summary of isotherm model parameters for Pb ions adsorption on n-CaHAP.

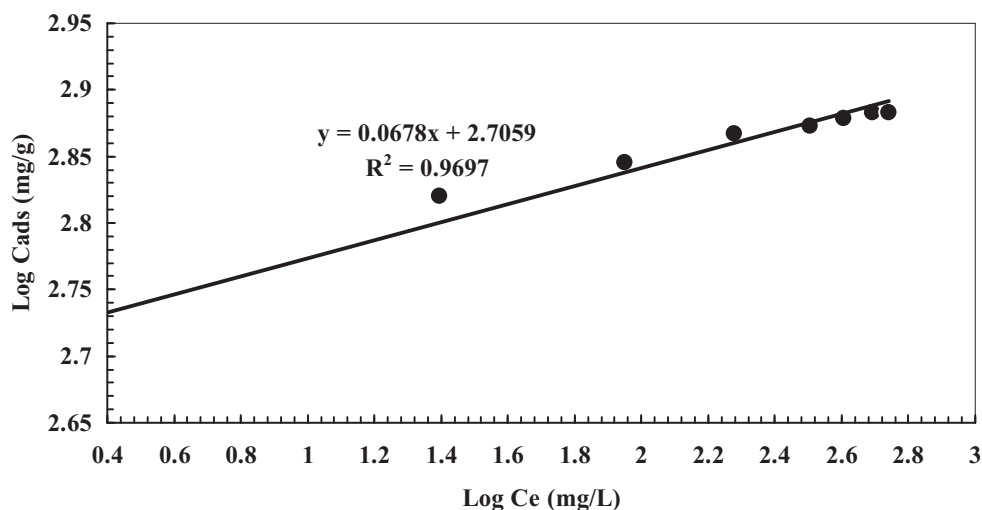| Metals	Langmuir model			Freundlich model		
	b L/mg	q_{max} (mg/g)	R^2	K_f	n	R^2
Lead ions	42.76	769.23	0.9998	508	14.75	0.969

Figure 10 Langmuir isotherm for lead ion adsorption onto n-CaHAP.

The simplified Freundlich equation is given by:

$$\log q_e = \log K_f + \frac{1}{n} \log C_e \tag{6}$$

where k_f and n are the Freundlich constants and are related to the adsorption capacity of the sorbent and the adsorption intensity.

The selection between Langmuir and Freundlich isotherms depends generally on the equilibrium data [62], where, the adsorption phenomena at the solid–liquid interface were commonly described by the adsorption isotherm model, and adsorption isotherms are an essential data source for practical design of adsorption systems and understanding of relation with adsorbent and adsorbate [63].

Langmuir and Freundlich isotherm parameters are listed in Table 1. Langmuir isotherm assumes monolayer adsorption, the R^2 value for lead ions was 0.999, which revealed the extremely good applicability of the Langmuir model to these adsorptions. The Freundlich model has commonly described the adsorption characteristics on the heterogeneous surface as an empirical equation based on adsorption on a heterogenous surface [64]. From Fig. 10 and Fig. 11, it can be concluded that the Langmuir isotherm is the best fit among other isotherms. The adsorption capacity of n-CaHAP was 769.23 mg Pb (II)/g of n-CaHAP which is similar to results of [65], they also found that the Langmuir isotherm is favorable and capacity of their nano-sized hydroxyapatite is found to be 357.14 mg Pb (II)/g.

Dubinin–Kaganer–Radushkevich (DKR) model is more broad than the Langmuir isotherm, because it does not suppose a homogeneous surface or constant sorption potential [66].

The DKR isotherm linear equation can be written as shown in Eq. (7)

$$\ln q_e = \ln X_m - \beta \varepsilon^2 \tag{7}$$

where q_e is the number of lead ions adsorbed per unit weight of the adsorbent (mol/g), X_m is the maximum sorption capacity, is the activity coefficient related to mean sorption energy, and ε is the Polanyi potential, which is equal to:
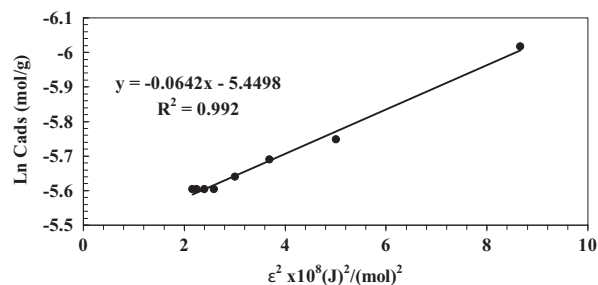

Figure 12 DKR sorption isotherm of lead ion onto n-CaHAP.

Figure 11 Freundlich isotherm for lead ion adsorption onto n-CaHAP.

Table 2 Summary of DKR model parameters for Pb ions adsorption on n-CaHAP.

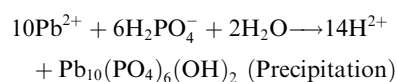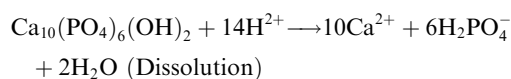| Metal	X_m (mol/g)	β (mol^2/J^2)	Sorption energy (E, kJ/mol)	Correlation coefficient R^2
Lead ions	5.449×10^{-3}	-0.0642×10^{-8}	27.9	0.992

$$\varepsilon = RT \ln \left(1 + \frac{1}{C_e}\right) \qquad (8)$$

where R is the gas constant (J/mol K) and T is the temperature (K). The saturation limit X_m may represent the total specific microspore volume of the sorbent. The sorption potential is generally varied according to the nature of sorbent and sorbate, but it is independent of the temperature [67]. The slope of the plot of ln q_e versus ε^2 gives (mol^2/J^2) and the intercept yields the sorption capacity, X_m (mol/g). The sorption space in the vicinity of a solid surface is characterized by a series of equipotential surfaces having the same sorption potential. The sorption energy can also be achieved using Eq. (9):

$$E = \frac{1}{\sqrt{-2\beta}} \qquad (9)$$

Fig. 12 represented by ln q_e against ε^2 for Pb (II) sorption onto n-CaHAP. Table 2 shows the DKR constants which are calculated from the slope of the line. It shows that, the E value is 27.9 kJ/mol for Pb (II) onto n-CaHAP. The E value is positive which indicates that the sorption process is endothermic.

Therefore, in order to interpret the mechanism of Pb (II) sorption by HAP from our result and from previous studies which have suggested that there are three types of reactions which may control Pb (II) sorption by HAP such as surface adsorption, cation substitution or precipitation. The first mechanism is the adsorption of Pb (II) ions on the HAP surfaces and following an ion exchange reaction between Pb (II) ions adsorbed and Ca^{+2} ions of HAP [68], while, Ma et al. [69] showed that HAP dissolution and hydroxypyromorphite (HP) precipitation were the main mechanisms for Pb (II) sorption by HAP. These chemical reactions can be described as follows:

$$Ca_{10}(PO_4)_6(OH)_2 + 14H^{2+} \longrightarrow 10Ca^{2+} + 6H_2PO_4^-$$
$$+ 2H_2O \text{ (Dissolution)}$$

$$10Pb^{2+} + 6H_2PO_4^- + 2H_2O \longrightarrow 14H^{2+}$$
$$+ Pb_{10}(PO_4)_6(OH)_2 \text{ (Precipitation)}$$

Also, the sorption mechanisms have been inferred by [70,71] who proved the type of mechanism by the values of molar ratios of cations bound by HAP to Ca desorbed from HAP which is less than 1 and this means that the dissolution and precipitation are the main mechanisms for Pb (II) adsorption by HAP. The previous studies are consistent with our selected three isotherm models which indicates that the mechanism of reaction type is chemisorption ($E > 16$ kJ/mol) as chemisorption is a chemical adsorption in which adsorption is caused by the formation of chemical bonds between the surface of solids (adsorbent) and Pb (II) (adsorbate). So the adsorption type can be explained as chemisorption than an ion exchange process. Also, several authors confirmed that dissolution and precipitation are the main mechanisms for Pb (II) adsorption by hydroxyapatite [72–75].

4. Conclusion

The calcium hydroxyapatite nanoparticles (n-CaHAP) could represent an economical source of sorbent for lead ions from wastewater. The sorption of lead ions on n-CaHAP was very rapid and the equilibrium was attained within 5 min. The kinetic experimental data were properly correlated with the second order kinetic model. The adsorption isotherm studies indicated that the correlation factors of the Langmuir isotherms are > 0.999. The maximum adsorption capacity (q_{max}) for Pb ions was 769.23 mg/g. The free energy (E) was 27.9 kJ/Mol which shows that the sorption process is endothermic and the mechanism of the reaction is by chemical adsorption.

References

[1] B. Volesky, Detoxification of metal-bearing effluents: biosorption for the next century, Hydrometallurgy 59 (2001) 203–216.

[2] L. Deng, Y. Su, H. Su, X. Wang, X. Zhu, Biosorption of copper(II) and lead(II) from aqueous solutions by nonliving green algae *Cladophora fascicularis*: equilibrium, kinetics and environmental effects, Adsorption 2 (2006) 267–277.

[3] P. King, N. Rakesh, S. Beenalahari, Y. Prasanna Kumar, Removal of lead from aqueous solution using *Syzygium cumini* L.: equilibrium and kinetic studies, J. Hazard. Mater. 142 (2007) 340–347.

[4] S. Davydova, Heavy metals as toxicants in big cities, Microchem. J. 79 (2005) 133–136.

[5] G. De la Rosa, H.E. Reynel-Avila, A. Bonilla-Petriciolet, I. Cano-Rodriguez, C. Velasco-Santos, A.L. Martínez-Hernández, Recycling poultry feathers for Pb (II) removal from wastewater: kinetic and equilibrium studies, Int. J. Chem. Biol. Eng. 1 (2008) 185–193.

[6] A. Naima, B. Mohamed, M. Hassiba, S. Zahra, Adsorption of lead from aqueous solution onto untreated orange barks, Chem. Eng. Trans. 32 (2013) 55–60.

[7] M.N.M. Ibrahim, W.S.W. Ngah, M.S. Norliyana, W.R.W. Daud, M. Rafatullah, O. Sulaiman, R. Hashim, A novel agricultural waste adsorbent for the removal of lead (II) ions from aqueous solutions, J. Hazard. Mater. 182 (2010) 377–385.

[8] H.S. Ibrahim, T.S. Jamila, E.Z. Hegazy, Application of zeolite prepared from Egyptian kaolin for the removal of heavy metals: II. Isotherm models, J. Hazard. Mater. 182 (2010) 842–847.

[9] H. Lalhruaitluanga, K. Jayaram, M.N.V. Prasad, K.K. Kumar, Lead (II) adsorption from aqueous solutions by raw and activated charcoals of *Melocanna baccifera* Roxburgh (bamboo): a comparative study, J. Hazard. Mater. 175 (2010) 311–318.

[10] S.W. Liao, C.I. Lin, L.H. Wang, Kinetic study on lead (II) ion removal by adsorption onto peanut hull ash, J. Taiwan Inst. Chem. Eng. 42 (2011) 166–172.

[11] T. Depci, A.R. Kul, Y. Önal, Competitive adsorption of lead and zinc from aqueous solution on activated carbon prepared from Van apple pulp: study in single- and multi-solute systems, Chem. Eng. J. 200–202 (2012) 224–236.

[12] M.R. Lasheen, N.S. Ammar, H.S. Ibrahim, Adsorption/desorption of Cd(II), Cu(II) and Pb(II) using chemically modified orange peel: equilibrium and kinetic studies, Solid State Sci. 14 (2012) 202–210.

[13] L. Mouni, D. Merabet, A. Bouzaza, L. Belkhiri, Adsorption of Pb(II) from aqueous solutions using activated carbon developed from Apricot stone, Desalination 276 (2011) 148–153.

[14] T.S. Anirudhan, S.S. Sreekumari, Adsorptive removal of heavy metal ions from industrial effluents using activated carbon derived from waste coconut buttons, J. Environ. Sci. 23 (2011) 1989–1998.

[15] B.J. Pan, B.C. Pan, W.M. Zhang, L. Lv, Q.X. Zhang, S.R. Zheng, Development of polymeric and polymer-based hybrid adsorbents for pollutants removal from waters, Chem. Eng. J. 151 (2009) 19–29.

[16] D. Ayhan, Heavy metal adsorption onto agro-based waste materials: a review, J. Hazard. Mater. 157 (2008) 220–229.

[17] A. Carbonell-Barrachina, R.D. Delaune, A. Jugsujinda, Phosphogypsum chemistry under highly anoxic conditions, Waste Manage. 22 (2002) 657–665.

[18] P. Bhawan, Guidelines for management and handling of phosphogypsum generated from phosphoric acid plants, CPCB. Available at < www.cpcb.in > (accessed on 19 June 2012).

[19] L. Reijnders, Cleaner phosphogypsum, coal combustion ashes and waste incineration ashes for application in building materials: a review, Build. Environ. 42 (2007) 1036–1042.

[20] A.A. Hanna, A.I.M. Akarish, S.M. Mousa, Phosphogypsum 1-mineralogical, thermogravimetric, chemical and infrared characterization, J. Mater. Sci. Technol. 15 (1999) 431–434.

[21] A.A. Hanna, Y.M. Abu-Ayana, S.M. Mousa, Phosphogypsum utilization as adhesive feller and composite materials, J. Mater. Sci. Technol. 16 (2000) 439–444.

[22] A.N. Hayati, H.R. Rezaie, S.M. Hosseinalipour, Preparation of poly (3-hydroxybutyrate)/nano-hydroxyapatite composite scaffolds for bone tissue engineering, Mater. Lett. 65 (2011) 736–739.

[23] K.R. Mohamed, S.M. Mousa, G.T. El Bassyouni, Fabrication of nano structural biphasic materials from phosphogypsum waste and their in vitro applications, Mater. Res. Bull. 50 (2014) 432–439.

[24] R. Murugan, S. Ramakrishna, Development of nanocomposites for bone grafting, Compos. Sci. Technol. 65 (2005) 2385–2405.

[25] M. Jarcho, C.H. Bolen, M.B. Thomas, J.F. Kay, Hydroxyapatite synthesis and characterization in dense polycrystalline form, J. Mater. Sci. 11 (1976) 2027–2035.

[26] J. Baton, A.J. Kadaksham, A. Nzihou, P. Singh, N. Aubry, Trapping heavy metals by using calcium hydroxyapatite and dielectrophoresis, J. Hazard. Mater. A139 (2007) 461–466.

[27] A. Mortimer, J. Lemaitre, Synthesis and thermal behavior of well-crystal size calcium-deficient phosphateapatite, J. Solid State Chem. 78 (1989) 215–219.

[28] S. Baillez, A. Nzihou, D. Bernache-Assolant, E. Champion, P. Sharrock, Removal of aqueous lead ions by hydroxyapatites: equilibria and kinetic processes, J. Hazard. Mater. 139 (2007) 443–446.

[29] M. Hadioui, P. Sharrock, M.O. Mecherri, V. Brumas, M. Fiallo, Reaction of lead ions with hydroxylapatite granules, Chem. Pap. 62 (2008) 516–521.

[30] J. Tan, M. Chen, J. Xia, Water-dispersible hydroxyapatite nanorods synthesized by a facile method, Appl. Surf. Sci. 255 (2009) 8774–8779.

[31] I.C. Huang, Y.B. Zhou, Z.M. Tang, X. Guo, Z.Y. Qian, S.B. Zhou, Synthesis of multifunctional Fe3O4 core/hydroxyapatite shell nanocomposites by biomineralization, Dalton Trans. 40 (2011) 5026–5031.

[32] B. Jokic, M. Mitered, V. Radmilovid, S. Drmanic, R. Petrovic, D. Janackovic, Synthesis and characterization of monetite and hydroxyapatite whiskers obtained by a hydrothermal method, Ceram. Int. 37 (2011) 167–173.

[33] D.P. Minh, N.D. Tran, A. Nzihou, P. Sharrock, Hydroxyapatite gel for the improved removal of Pb^{2+} ions from aqueous solution, Chem. Eng. J. 232 (2013) 128–138.

[34] D.P. Minh, N.D. Tran, A. Nzihou, P. Sharrock, Calcium phosphate based materials starting from calcium carbonate and orthophosphoric acid for the removal of lead(II) from an aqueous solution, Chem. Eng. J. 243 (2014) 280–288.

[35] S.M. Mousa, A.A. Hanna, Synthesis of nano-crystalline hydroxyapatite and ammonium sulfate from phosphogypsum waste, Mater. Res. Bull. 48 (2013) 823–828.

[36] A.E. Greenberg, L.S. Clesceri, A.D. Eaton, Standard Methods for the Examination of Water & Wastewater, 22nd ed., Washington, 1999.

[37] I. Mobasherpour, E. Salahi, M. Pazouki, Potential of nano crystalline hydroxyapatite for lead (II) removal from aqueous solutions: thermodynamic and adsorption isotherm study, Afr. J. Pure Appl. Chem. 5 (2011) 383–392.

[38] I. Mobasherpour, E. Salahi, M. Pazouki, Removal of nickel (II) from aqueous solutions by using nano-crystalline calcium hydroxyapatite, J. Saudi Chem. Soc. 15 (2011) 105–112.

[39] Y. Bessekhouad, D. Robert, J.-V. Weber, N. Chaoui, Effect of alkaline-doped TiO2 on photocatalytic efficiency, J. Photochem. Photobiol., A 167 (2004) 49–57.

[40] V.K. Gupta, S. Agarwal, T.A. Saleh, Synthesis and characterization of alumina-coated carbon nanotubes and their application for lead removal, J. Hazard. Mater. 185 (2011) 17–23.

[41] I. Sneddon, H. Garelick, E. Valsami-Jones, An investigation into arsenic (V) removal from aqueous solutions by hydroxylapatite and bone-char, Mineral. Mag. 69 (2005) 769–780.

[42] D. Mohan, C. Pittman, Arsenic removal from water/wastewater using adsorbents – a critical review, J. Hazard. Mater. 142 (2007) 1–53.

[43] H. Hasan, P. Srivastava, M. Talatb, Biosorption of lead using immobilized Aeromonas hydrophila biomass in up flow column system: factorial design for process optimization, J. Hazard. Mater. 177 (2010) 312–322.

[44] M.A.M. Khraisheh, Y.S. Al-degs, W.A.M. Mcminn, Remediation of wastewater containing heavy metals using raw and modified diatomite, Chem. Eng. J. 99 (2004) 177–184.

[45] M.A. Al-Ghouti, M.A.M. Khraisheh, S.J. Allen, M.N. Ahmad, The removal of dyes from textile wastewater: a study of the physical characteristics and adsorption mechanisms of diatomaceous earth, J. Environ. Manage. 69 (2003) 229–238.

[46] G. Ghanizadeh, G. Asgari, Adsorption kinetic and isotherm of methylene blue and its removal from aqueous solution using bone charcoal, React. Kinet. Mech. Catal. 102 (2011) 127–142.

[47] G.E. Jai Poinern, K.G. Malay, Y.J. Ng, B.I.T. Touma, Defluoridation behavior of nanostructured hydroxy-apatite synthesized through an ultrasonic and microwave combined technique, J. Hazard. Mater. 185 (2011) 29–37.

[48] D. Liao, W. Zheng, X. Li, Q. Yang, X. Yueb, L. Guo, G. Zeng, Removal of lead(II) from aqueous solutions using carbonate hydroxyapatite extracted from eggshell waste, J. Hazard. Mater. 177 (2010) 126–130.

[49] A. Mittal, J. Mittal, A. Malviya, V.K. Gupta, Removal and recovery of Chrysoidine Y from aqueous solutions by waste materials, J. Colloid Interface Sci. 344 (2010) 497–507.

[50] N.A. Oladoja, C.O. Aboluwoye, Y.B. Oladimeji, Kinetics and isotherm studies on methylene blue adsorption onto ground palm kernel coat, Turk. J. Eng. Environ. Sci. 32 (2008) 303–312.

[51] S. Lagergren, Zur theorie der sogenannten adsorption geloster stoffe, K S V, Handlingar 24 (1898) 1–39.

[52] Y.S. Ho, G. Mckay, D.J. Wase, C.F. Foster, Study of the sorption of divalent metal ions on to peat, Adsorpt. Sci. Technol. 18 (2000) 639–650.

[53] L. Abramian, H. El-Rassy, Adsorption kinetics and thermodynamics of azo-dye orange II onto highly porous titania aerogel, Chem. Eng. J. 150 (2009) 403–410.

[54] A.U. Itodo, F.W. Abdulrahman, L.G. Hassan, S.A. Maigandi, U.O. Happiness, Diffusion mechanism and kinetics of biosorption of textile dye by H_3PO_4 and $ZnCl_2$ impregnated poultry wastes sorbents, Int. J. Nat. Appl. Sci. 5 (2009) 7–12.

[55] V. Shrihari, S. Madhan, A. Das, Kinetics of phenol sorption by raw agrowastes, Appl. Sci. 6 (2005) 47–50.

[56] J. Biyan, S. Fei, G. Hu, S. Zheng, Q. Zhang, Z. Xu, Adsorption of methyl tert-butyl ether (MTBE) from aqueous solution by porous polymeric adsorbent, J. Hazard. Mater. 161 (2009) 81–87.

[57] A.E. Nemr, Potential of pomegranate husk carbon for Cr (VI) removal from wastewater: kinetic and isotherm studies, J. Hazard Mater. 161 (2009) 132–141.

[58] T.K. Naiya, A.K. Bhattacharya, S.K. Das, Adsorption of Cd (II) and Pb (II) from aqueous solutions on activated alumina, J. Colloid Interface Sci. 333 (2009) 14–26.

[59] M.M. Rao, G.P. Rao, K. Seshaiah, N.V. Choudary, M.C. Wang, Activated carbon from Ceiba pentandra hulls, an agricultural waste, as an adsorbent in the removal of lead and zinc from aqueous solutions, Waste Manage. 28 (2008) 849–858.

[60] L. Su-Hsia, J. Ruey-Shin, Adsorption of phenol and its derivatives from water using synthetic resins and low-cost natural adsorbents: a review, J. Environ. Manage. 90 (2009) 1336–1349.

[61] I. Langmuir, The constitution and fundamental properties of solids and liquids, J. Am. Chem. Soc. 38 (1916) 2221–2295.

[62] S. Schiewer, B. Volesky, Environmental Microbe–Metal Interactions, ASM Press, Washington, 2000, pp. 329–362.

[63] S. Saygideger, O. Gulnaz, E.S. Istifli, N. Yucel, Adsorption of Cd(II), Cu(II) and Ni(II) ions by Lemna minor L.: effect of physicochemical environment, J. Hazard. Mater. 126 (2005) 96–104.

[64] N.D. Hutson, R.T. Yang, Theoretical basis for Dubinin–Radushkevich (D–R) adsorption isotherm equation, Adsorption 3 (1997) 189–195.

[65] S.T. Ramesh, N. Rameshbabu, R. Gandhimathi, M. Srikanth Kumar, P.V. Nidheesh, Adsorptive removal of Pb(II) from aqueous solution using nano-sized hydroxyapatite, Appl. Water Sci. 3 (2013) 105–113.

[66] A. Kilislioglu, B. Bilgin, Thermodynamic and kinetic investigations of uranium adsorption on amberlite IR-118H resin, Appl. Radiat. Isot. 50 (2003) 155–160.

[67] S.A. Khan, U.R. Rehman, M.A. Khan, Adsorption of chromium (III), chromium (VI) and silver (I) on bentonite, Waste Manage. 15 (1995) 271–278.

[68] T. Suzuki, K. Ishigaki, M. Miyake, Synthetic hydroxyapatites as inorganic cation exchangers exchange characteristics of Pb(II) ions, J. Chem. Soc., Faraday Trans. 80 (1984) 3157–3165.

[69] Q.Y. Ma, S.J. Traina, T.J. Logan, J.A. Ryan, Effect of aqueous Al, Cd, Cu, Fe(II), Ni, and Zn on Pb(II) immobilization by hydroxyapatite, Environ. Sci. Technol. 28 (1994) 1219–1228.

[70] M. Aklil, M. Mouflih, S. Sebti, Removal of heavy metal ions from water by using calcined phosphate as a new adsorbent, J. Hazard. Mater. 112 (2004) 183–190.

[71] A. Corami, S. Mignardi, V. Ferrini, Copper and zinc decontamination from single- and binary-metal solutions using hydroxyapatite, J. Hazard. Mater. 146 (2007) 164–170.

[72] S.H. Lin, R.S. Juang, Heavy metal removal from water by sorption using surfactant-modified montmorillonite, J. Hazard. Mater. 92 (2002) 315–326.

[73] C.C. Wang, L.C. Juang, C.K. Lee, T.C. Hsu, J.F. Lee, H.P. Chao, Effects of exchanged surfactant cations on the pore structure and adsorption characteristics of montmorillonite, J. Colloid Interface Sci. 280 (2004) 27–35.

[74] B.S. Krishna, D.S.R. Murty, B.S. Jai Prakash, Thermodynamics of chromium (VI) anionic species sorption onto surfactant-modified montmorillonite clay, J. Colloid Interface Sci. 229 (2000) 230–236.

[75] R.V. Ghita, S.L. Iconaru, C.L. Popa, A. Costescu, P.L. Coustumer, M. Motelica-Heino, C.S. Ciobanu, Tetraethyl orthosilicate coated hydroxyapatite powders for lead ions removal from aqueous solutions, J. Nanomater. 1 (2014) 1–7.